



# Degradation of acidic aqueous solutions of the diazo dye Congo Red by photo-assisted electrochemical processes based on Fenton's reaction chemistry



Aline Maria Sales Solano<sup>a</sup>, Sergi Garcia-Segura<sup>b</sup>, Carlos Alberto Martínez-Huitle<sup>a,\*\*</sup>, Enric Brillas<sup>b,\*</sup>

<sup>a</sup> Laboratório de Eletroquímica Ambiental e Aplicada, Instituto de Química, Universidade Federal do Rio Grande do Norte, Lagoa Nova – CEP 59.072-900, RN, Brazil

<sup>b</sup> Laboratori d'Electroquímica dels Materials i del Medi Ambient, Departament de Química Física, Facultat de Química, Universitat de Barcelona, Martí i Franquès 1-11, 08028 Barcelona Spain

## ARTICLE INFO

### Article history:

Received 28 November 2014

Received in revised form 13 January 2015

Accepted 17 January 2015

Available online 20 January 2015

### Keywords:

Congo Red

Electro-Fenton

Photoelectro-Fenton

Solar light

Water treatment

## ABSTRACT

The degradation of solutions with 0.260 mM of the diazo dye Congo Red at pH 3.0 has been studied by electrochemical advanced oxidation processes (EAOPs) like anodic oxidation with electrogenerated  $\text{H}_2\text{O}_2$  (AO- $\text{H}_2\text{O}_2$ ), electro-Fenton (EF) and photoelectro-Fenton (PEF) with a 6 W UVA light. Experiments were made in a 100 mL stirred tank reactor with a boron-doped diamond (BDD) anode and an air-diffusion cathode at constant current density ( $j$ ). In these systems, organics were mainly destroyed by  $\bullet\text{OH}$  formed at the anode surface from water oxidation and/or in the bulk from Fenton's reaction between added  $\text{Fe}^{2+}$  and cathodically generated  $\text{H}_2\text{O}_2$ . The oxidation power of the EAOPs increased in the sequence AO- $\text{H}_2\text{O}_2 < \text{EF} < \text{PEF}$ . Almost total mineralization was attained after 360 min of PEF at  $j \geq 66.7 \text{ mA cm}^{-2}$  due to the parallel photolytic action of UVA light. In all the EAOPs, increasing  $j$  enhanced the degradation process, but with a loss of mineralization current efficiency and higher energy consumption. Congo Red decay always obeyed a pseudo-first-order kinetics. The study of the Congo Red degradation in a 2.5 L solar flow plant with a Pt/air-diffusion cell confirmed the viability of the solar PEF (SPEF) treatment at industrial scale. Optimum conditions were found for 0.260 mM of Congo Red with 0.50 mM  $\text{Fe}^{2+}$  at  $100 \text{ mA cm}^{-2}$ , yielding almost total mineralization in 240 min with about 49% current efficiency and  $0.45 \text{ kWh (g DOC)}^{-1}$  energy consumption. LC-MS analysis of treated solutions allowed the identification of 21 aromatic intermediates and 13 hydroxylated derivatives, including diazo, monoazo, biphenyl, benzene, naphthalene and phthalic acid compounds. Tartatic, tartaric, acetic, oxalic and oxamic acids were detected as final carboxylic acids in all the EAOPs. The fast photodecarboxylation of the  $\text{Fe(III)-carboxylate}$  complexes explained the higher oxidation ability of the photo-assisted methods of PEF and SPEF. The initial N of the dye was mainly lost as N-volatile products and mineralized to  $\text{NO}_3^-$  ion and in lesser extent to  $\text{NH}_4^+$  ion, whereas its initial S was converted into  $\text{SO}_4^{2-}$  ion.

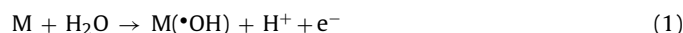
© 2015 Elsevier B.V. All rights reserved.

## 1. Introduction

Recently, electrochemical advanced oxidation processes (EAOPs) have received great attention for the remediation of toxic and biorefractory organic pollutants in acidic waters [1–4]. In these emerging and environmentally friendly technologies, the organic matter is mineralized by mediated oxidation with reactive oxygen species (ROS), primordially with hydroxyl radical ( $\bullet\text{OH}$ )

generated in situ at the anode surface at high current and/or in the bulk from Fenton's reaction chemistry.  $\bullet\text{OH}$  is the second strongest oxidant known, after fluorine, and its high standard redox potential ( $E^\circ = 2.80 \text{ V/SHE}$ ) allows complete combustion of most organics to  $\text{CO}_2$ , inorganic ions and water [4–6].

The most common EAOP is anodic oxidation (AO), in which water is oxidized to  $\text{O}_2$  at an anode (M) with high  $\text{O}_2$ -overpotential to generate adsorbed hydroxyl radical  $\text{M}(\bullet\text{OH})$  as intermediate from Reaction (1) [1,7,8].



Among the anodes currently used in AO, boron-doped diamond (BDD) thin-film electrodes are preferred because their weak

\* Corresponding author. Tel.: +34 934021223; fax: +34 934021231.

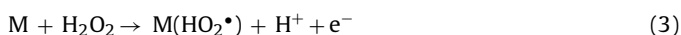
\*\* Corresponding author.

E-mail addresses: [carlosmh@quimica.ufrn.br](mailto:carlosmh@quimica.ufrn.br) (C.A. Martínez-Huitle), [brillas@ub.edu](mailto:brillas@ub.edu) (E. Brillas).

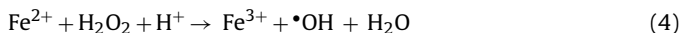
BDD-•OH interaction and greater O<sub>2</sub>-overpotential leads to the generation of higher amounts of reactive physisorbed BDD(•OH) radicals that mineralize more effectively aromatics and aliphatic contaminants than other anodes as Pt and PbO<sub>2</sub> [7–16]. When H<sub>2</sub>O<sub>2</sub> is additionally produced from the two-electron reduction of injected O<sub>2</sub> by Reaction (2) in an undivided cell, the EAOP is called AO with electrogenerated H<sub>2</sub>O<sub>2</sub> (AO-H<sub>2</sub>O<sub>2</sub>) [4]:



A high efficiency of Reaction (2) is found using carbonaceous cathodes like activated carbon fiber [17], carbon or graphite felts [15,18–21], carbon sponge [22], carbon nanotubes [23], carbon-polytetrafluoroethylene (PTFE) gas (O<sub>2</sub> or air) diffusion [24–27] and BDD [28–30]. An advantage of the AO-H<sub>2</sub>O<sub>2</sub> process with a carbon-PTFE air-diffusion cathode is the minimization of possible cathodic reduction of organics [31]. Moreover, other weak ROS like hydroperoxyl radical (HO<sub>2</sub>•) can be generated at the anode from H<sub>2</sub>O<sub>2</sub> oxidation as follows:



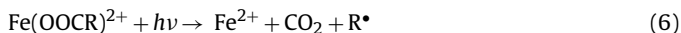
Indirect EAOPs with H<sub>2</sub>O<sub>2</sub> electrogeneration based on Fenton's reaction chemistry are usually more potent than AO-H<sub>2</sub>O<sub>2</sub> [2,4,6]. The most typical of these EAOPs is electro-Fenton (EF) in which low amounts of added Fe<sup>2+</sup> ion react with generated H<sub>2</sub>O<sub>2</sub> to yield Fe<sup>3+</sup> ion and homogeneous •OH in the bulk via Fenton's Reaction (4) with optimum pH 2.8 [15,17–22,24,26–29,31]:



An advantage of Reaction (4) is that can be propagated from Fe<sup>2+</sup> regeneration, which mainly takes place by cathodic reduction of Fe<sup>3+</sup> [18,22]. In an undivided cell, the EF process involves the simultaneous destruction of the organic matter by M(•OH) produced at the anode from Reaction (1) and •OH formed in the bulk from Reaction (4), along with a slower removal by other weaker ROS like H<sub>2</sub>O<sub>2</sub> and HO<sub>2</sub>• [2,4]. Several authors have shown a quicker faster degradation of organics in the cathodic compartment of a divided cell compared to an undivided one as a result of the higher accumulation of H<sub>2</sub>O<sub>2</sub> in the former system [32,33]. The formation of stable Fe(III)-carboxylate complexes, only slowly destroyed by BDD(•OH), as final products of aromatics degradation is the main drawback to achieve total mineralization when a gas-diffusion cathode is utilized in an undivided cell [6,34]. To solve this problem, the photoelectro-Fenton (PEF) process by simultaneously irradiating the solution under EF treatment with UVA light can be applied [24,26,27,35]. The action of UVA light is complex and can involve the photolysis of Fe(OH)<sup>2+</sup>, the preferential Fe<sup>3+</sup> species at pH close to 3, regenerating more Fe<sup>2+</sup> ion and producing more •OH from photo-Fenton Reaction (5):



Moreover, UVA radiation can enhance the mineralization process from the photodecarboxylation of generated Fe(III)-carboxylate complexes with Fe<sup>2+</sup> regeneration by the general Reaction (6):



The main drawback of PEF is the high energetic requirements of the artificial UVA lamp used. Our group has proposed the alternative use of sunlight as inexpensive and renewable energy source in the so-called solar PEF (SPEF) process, which has been tested for a small number of aromatic pollutants [25,26,31,36,37]. It has been found that the potent UV radiation of sunlight makes SPEF more viable than EF for organics mineralization. Hence, the good oxidation ability of SPEF needs to be confirmed for a higher number of pollutants to show its possible application at industrial scale.

There is a growing concern about the environmental problems caused by the discharge of large volumes of dyeing industrial effluents into water bodies [38]. The color of such effluents creates an esthetic problem that discourages the downstream use of waste water [4,39]. The most utilized synthetic dyes are azo dyes, which represent about 70% of annual consumption of these compounds [4,40]. Azo dyes contain one or various azo groups (N=N–) as chromophore, linked to aromatic moieties with lateral groups like –OH and –SO<sub>3</sub>H. They are largely persistent in the aquatic environment because of their inefficient removal by conventional biological and physicochemical methods in municipal waste water treatment plants. It has been found that these pollutants are toxic to living beings [41,42], also possessing carcinogenic, mutagenic and bactericide properties [38]. For this reason, many research efforts are being focused to develop efficient processes to remove azo dyes from waters.

EAOPs like AO, EF, PEF and SPEF have been successfully applied to the treatment of several monoazo dye solutions [17,18,20–23,28,29,31,37]. However, less is known about the degradative behavior of diazo dye solutions by these methods, only being reported a limited number of articles on the use of AO [43,44] and EF [27,45], but the oxidative action of the most potent PEF and SPEF processes have not yet been tested. To gain a better understanding on the oxidation ability of both photo-assisted electrochemical methods, we have undertaken a study on the mineralization of the diazo dye Congo Red (disodium salt of C<sub>32</sub>H<sub>22</sub>N<sub>6</sub>O<sub>6</sub>S<sub>2</sub><sup>2–</sup>, *M* = 696.66 g mol<sup>–1</sup>, λ<sub>max</sub> = 503 nm) by EAOPs. This compound is currently used as pH indicator and to stain microscopic preparates, especially as a cytoplasm and erythrocyte stain. Moreover, the birefringence of its stained preparates under polarized light indicates the presence of amyloid fibrils. Total mineralization of 600 mL of neutral aqueous solutions of Congo Red up to 500 mg L<sup>–1</sup> in 5 g L<sup>–1</sup> Na<sub>2</sub>SO<sub>4</sub> has been reported using a bench-scale flow plant with a BDD/stainless steel reactor of 78 cm<sup>2</sup> electrode area after the consumption of 90 A h L<sup>–1</sup> operating at 30 mA cm<sup>–2</sup> [43]. The application of the EF process to 125 mL of a mixture with 0.25 mM of this dye and the same content of Yellow Dimaren and methyl orange at pH 3.0 and 0.5 mM Fe<sup>3+</sup> using a Pt/carbon-felt cell at 40 mA revealed that Congo Red decayed according to a pseudo-first-order kinetics, but only 89% mineralization of the dyes mixture was attained after consuming a charge of 10,000 C [45]. In these works, however, products of Congo Red were not determined.

This paper presents the comparative decolorization, dye removal and mineralization of a 0.260 mM Congo Red solution at pH 3.0 by AO-H<sub>2</sub>O<sub>2</sub>, EF and PEF using a stirred BDD/air-diffusion tank reactor. The role of the different generated oxidizing agents was clarified from the influence of the applied current density (*j*) on each EAOP. The study was further extended to the SPEF process using a solar flow plant equipped with a Pt/air-diffusion filter-press cell. The effect of *j* and dye and Fe<sup>2+</sup> concentrations on the SPEF treatment was examined to know its optimum operating conditions. Aromatic intermediates were identified by liquid chromatography (LC)–mass spectrometry (MS). For all the EAOPs tested, the dye decay, the evolution of final short-linear carboxylic acids and released inorganic ions were determined by chromatographic techniques.

## 2. Experimental

### 2.1. Chemicals

Commercial Congo Red dye (85% purity, with the rest of inorganic ions for stabilization) was purchased from Sigma–Aldrich and used as received. Analytical grade anhydrous sodium sulfate

used as background electrolyte and heptahydrated iron(II) sulfate used as catalyst for Fenton's reaction were purchased from Fluka and Sigma–Aldrich, respectively. Carboxylic acids, other chemicals and solvents used in chromatographic techniques were of HPLC, LC–MS and analytical grade purchased from Sigma–Aldrich, Lancaster, Merck and Panreac. All solutions were prepared with high-purity water obtained from a Millipore Milli-Q system (resistivity > 18 MΩ cm at 25 °C). Analytical grade sulfuric acid from Merck was used to adjust the initial solution pH to 3.0.

## 2.2. Electrolytic systems

Electrolytic trials at lab scale by AO- H<sub>2</sub>O<sub>2</sub>, EF and PEF were carried out in an open and undivided two-electrode cell of 100 mL capacity with an external jacket for the circulation of thermostated water. The anode was a 3 cm<sup>2</sup> BDD thin film supplied by Adamant Technologies (La-Chaux-de-Fonds, Switzerland) and the cathode was a 3 cm<sup>2</sup> carbon-PTFE air-diffusion electrode from E-TEK (Somerset, NJ, USA), separated about 1 cm. The cathode was mounted as described elsewhere [24] and was fed with air pumped at a flow rate of 300 mL min<sup>-1</sup> for H<sub>2</sub>O<sub>2</sub> generation from Reaction (2). All the experiments were carried out with 100 mL of solutions containing 0.260 mM Congo Red in 0.05 M Na<sub>2</sub>SO<sub>4</sub> as background electrolyte at pH 3.0 operating at constant *j* provided by an Amel 2053 potentiostat-galvanostat. In EF and PEF, 0.50 mM Fe<sup>2+</sup> was added to the solution as catalyst. The solution pH and the Fe<sup>2+</sup> content were chosen because they are optimal for similar treatments of other aromatics [18,22,26,27,31]. The solution was maintained at 35.0 °C, which is the maximum temperature that can be attained in the cell without significant water evaporation, and was stirred with a magnetic bar at 800 rpm to ensure homogeneity in solution and the mass transport of reactants toward/from the electrodes. In PEF, the solution was irradiated with an UVA light provided by a Philips 6-W black light blue tube lamp with wavelengths of 320–400 nm and λ<sub>max</sub> = 360 nm. The lamp was placed at 7 cm above solution and supplied 5 W m<sup>-2</sup>, as detected with a Kipp & Zonen CUV 5 global UV radiometer. Before the treatments, the electrodes were polarized in 100 mL of 0.05 M Na<sub>2</sub>SO<sub>4</sub> at 100 mA cm<sup>-2</sup> for 180 min to remove the impurities of the BDD anode surface and activate the air-diffusion cathode.

A scheme of the 2.5 L batch recirculation flow plant built-up by us to carry out the SPEF degradations has been reported elsewhere [25]. In each assay, the Congo Red solution introduced into the reservoir was recirculated through the plant using a centrifugal pump at a flow rate of 200 L h<sup>-1</sup> regulated with a flowmeter and its temperature was kept at 35 °C by two heat exchangers connected to a water bath. The liquid flow rate was the maximal provided by the pump and was chosen because organics degradation is accelerated with increasing this parameter due to the concomitant enhancement of their mass transfer [46]. The solution passed through an undivided filter-press reactor with 20 cm<sup>2</sup> electrodes separated 1.2 cm, further circulating through the solar photoreactor before returning to the reservoir. The electrochemical cell was equipped with a Pt sheet anode of 99.99% purity from SEMPISA (Barcelona, Spain) and a carbon-PTFE air-diffusion cathode from E-TEK. The cathode was in contact with a gas chamber fed with atmospheric air at an overpressure of about 8.6 kPa regulated with a back-pressure gauge to continuously produce H<sub>2</sub>O<sub>2</sub>. A constant *j* was provided to the cell by an Agilent 6552A DC power supply, directly measuring the applied potential difference. The solar photoreactor consisted of a 24 cm × 24 cm × 2.5 cm polycarbonate box with a mirror at the bottom and inclined 41° to best collect the incident sun rays. The SPEF trials started from noon in sunny and clear days during the summer of 2014 in the University of Barcelona, Spain (latitude 41°21'N, longitude 2°10'E). The average UV irradiation intensity (300–400 nm) was 30–32 W m<sup>-2</sup>, as determined

with a Kipp & Zonen CUV 5 radiometer. The air-diffusion cathode was previously activated by electrolyzing 2.5 L of 0.05 M Na<sub>2</sub>SO<sub>4</sub> at pH 3.0 and 150 mA cm<sup>-2</sup> for 240 min.

## 2.3. Instruments and analytical procedures

The solution pH was determined by a Crison GLP 22 pH-meter. The samples withdrawn from electrolyzed solutions by EF, PEF and SPEF were alkalized to stop the mineralization process and filtered with 0.45 μm PTFE filters purchased from Whatman before analysis. The decolorization of Congo Red solutions was monitored from their absorbance (*A*) decay at the maximum visible wavelength of λ<sub>max</sub> = 503 nm using a Shimadzu 1800 UV–vis spectrophotometer thermostated at 35 °C. The percentage of color removal or decolorization efficiency was calculated by Eq. (7) [2,4]:

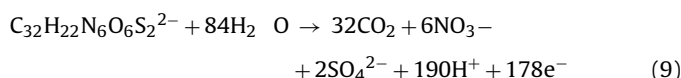
$$\% \text{Color removal} = \frac{A_0 - A_t}{A_0} 100 \quad (7)$$

where *A*<sub>0</sub> and *A*<sub>*t*</sub> are the absorbance at initial time and time *t* at λ<sub>max</sub> = 503 nm, respectively.

The mineralization of Congo Red solutions was monitored from their DOC (dissolved organic carbon) abatement, determined on a Shimadzu VCSN total organic carbon (TOC) analyzer. Reproducible DOC values with an accuracy of ±1% were obtained by injecting 50 μL aliquots into the analyzer. From the DOC decay, the mineralization current efficiency (MCE) at current *I* (in A) and given time *t* (in h) for each trial was estimated by Eq. (8) [37]:

$$\text{MCE}(\%) = \frac{nFV_s \Delta(\text{DOC})_{\text{exp}}}{4.32 \times 10^7 \text{ mlt}} 100 \quad (8)$$

where *F* is the Faraday constant (96,487 C mol<sup>-1</sup>), *V*<sub>s</sub> is the solution volume (in L), Δ(DOC)<sub>exp</sub> is the experimental DOC decay (in mg L<sup>-1</sup>), 4.32 × 10<sup>7</sup> is a conversion factor (3600 s h<sup>-1</sup> × 12000 mg C mol<sup>-1</sup>) and *m* is the number of carbon atoms of Congo Red (32 atoms). The *n*-value is the number of electrons involved in the total combustion of the dye and was taken as 178 assuming the main formation of nitrate and sulfate ions from Reaction (9), as discussed below.



Total nitrogen (TN) corresponding to all *N*-species present in solution was determined on a Shimadzu TNM-1 module coupled to the above TOC analyzer. The specific energy consumption per unit DOC mass (EC<sub>DOC</sub>) was determined as follows [37]:

$$\text{EC}_{\text{DOC}}(\text{kWh}(\text{gDOC})^{-1}) = \frac{E_{\text{cell}} \text{It}}{V_s \Delta(\text{DOC})_{\text{exp}}} \quad (10)$$

where *E*<sub>cell</sub> is the average potential difference of the cell (in V).

The dye decay was followed by reversed-phase HPLC using a waters 600 LC fitted with a waters Spherisorb ODS C18 5 μm (150 mm × 4.6 mm (i.d.)) column at 35 °C, and coupled with a waters 996 photodiode array detector set at λ = 503 nm. Generated carboxylic acids were detected by ion-exclusion HPLC using the above LC fitted with a Bio-Rad Aminex HPX 87H (300 mm × 7.8 mm (i.d.)) column at 35 °C and the photodiode array detector selected at λ = 210 nm. These measurements were made by injecting 20 μL aliquots into the LC and with a mobile phase constituted of a 40:60 (v/v) acetonitrile/water (2.4 mM *n*-butylamine) mixture at 0.4 mL min<sup>-1</sup> for reversed-phase HPLC and of 4 mM H<sub>2</sub>SO<sub>4</sub> at 0.6 mL min<sup>-1</sup> for ion-exclusion HPLC. Ammonium, nitrate and sulfate ions in treated solutions were analyzed by ion chromatography by injecting 25 μL aliquots into a Shimadzu 10Avp LC coupled to a Shimadzu CDD 10Avp conductivity detector. The NH<sub>4</sub><sup>+</sup> content was obtained using a Shodex IC YK-421 (125 mm × 4.6 mm

(i.d.) cationic column at 40 °C and a mobile phase of 24.2 mM boric acid, 5.0 mM tartaric acid, 1.5 mM 18-crown-6 and 2.0 mM 2,6-pyridinedicarboxylic solution at 1.0 mL min<sup>-1</sup>. The NO<sub>3</sub><sup>-</sup> and SO<sub>4</sub><sup>2-</sup> concentrations were determined with a Shim-Pack IC-A1S (100 mm × 4.6 mm (i.d.)) anionic column at 40 °C using a mobile phase composed of 2.6 mM phthalic acid and 2.4 mM tris(hydroxymethyl) aminomethane (pH 4.0) at 1.5 mL min<sup>-1</sup>.

Aromatic intermediates formed at short SPEF trials of a 0.260 mM Congo Red solution at 100 mA cm<sup>-2</sup> were identified by LC-MS using a Shimadzu SIL-20AC LC filled with a Teknokroma Mediterranean Sea C-18 3 μm (15 mm × 0.46 mm (i.d.)) column at 30 °C and coupled to a Shimadzu LCMS-2020 MS. The MS operated in negative mode with electrospray source ionization (ESI), by applying 4.5 kV interface voltage and 60 V Q-array RF voltage. The DL temperature was 250 °C and pure N<sub>2</sub> was used as nebulizing and dryer gas. Mass spectra were collected in the *m/z* range of 50–900 using both, total ion current (TIC) and selected ion (SIM) acquisition. To do this analysis, 20 μL aliquots were filtered with a Millipore filter of 0.22 μm and injected into the LC, using a 50:50 (v/v) acetonitrile/water (5 mM ammonium acetate) mixture at 0.2 mL min<sup>-1</sup> as mobile phase.

### 3. Results and discussion

#### 3.1. Comparative degradation of Congo Red by AO- H<sub>2</sub>O<sub>2</sub>, EF and PEF in a stirred tank reactor

Comparative assays were made to clarify the oxidation ability and the role of oxidizing agents for the AO-H<sub>2</sub>O<sub>2</sub>, EF and PEF treatments of 100 mL of a 0.260 mM Congo Red solution (corresponding to 100 mg L<sup>-1</sup> DOC) in 0.05 M Na<sub>2</sub>SO<sub>4</sub> at pH 3.0 and different *j* values between 16.7 and 100 mA cm<sup>-2</sup> for 360 min. In EF and PEF, 0.50 mM Fe<sup>2+</sup> was added as catalyst. In all these trials, the solution pH was not regulated because it was practically unchanged, decreasing up to a value of 2.7–2.8 as maximum, suggesting the formation of acidic products like short-chain carboxylic acids [2–4].

Fig. 1a shows the change of the percentage of color removal at λ<sub>max</sub> = 503 nm with electrolysis time for the EAOPs tested at *j* = 100 mA cm<sup>-2</sup>, showing the same plots for both EF and PEF processes. While 93% of color disappeared after 360 min of AO-H<sub>2</sub>O<sub>2</sub>, total decolorization was rapidly achieved in only 80–90 min of EF or PEF treatments. The low decolorization rate for the former process can be ascribed to the slow reaction of the dye with BDD(•OH) radical formed from Reaction (1), whereas the much quicker color removal for the two latter ones can be related with its more rapid reaction with additional •OH produced in the bulk from Fenton's Reaction (4). The fact that similar decolorization efficiency was achieved for both EF and PEF processes is indicative of a poor contribution of photo-Fenton Reaction (5) to •OH generation.

The aforementioned behavior was corroborated by determining the concentration abatement of Congo Red by reversed-phase HPLC, where it exhibited a well-defined peak at retention time (*t<sub>r</sub>*) of 5.14 min. As can be seen in Fig. 1b, the dye was completely removed from the solution in about 80 min for AO-H<sub>2</sub>O<sub>2</sub> and in only 40 min for EF and PEF due to the more powerful oxidative action of •OH produced in the bulk. Comparison of Fig. 1a and b allows concluding that much longer time was required to decolorize the solution than for the disappearance of the starting dye. This suggests that the decolorization process involves the generation of colored aromatic products with a significant absorbance at the maximum wavelength of 503 nm of the dye, which are more slowly destroyed by BDD(•OH) and/or •OH, as also observed in the degradation of several monoazo dyes by EAOPs [24,27,36]. Kinetic analysis of the above concentration decays showed a good agreement with a pseudo-first-order reaction of Congo Red as depicted in the inset panel of Fig. 1b. From the linear correlations

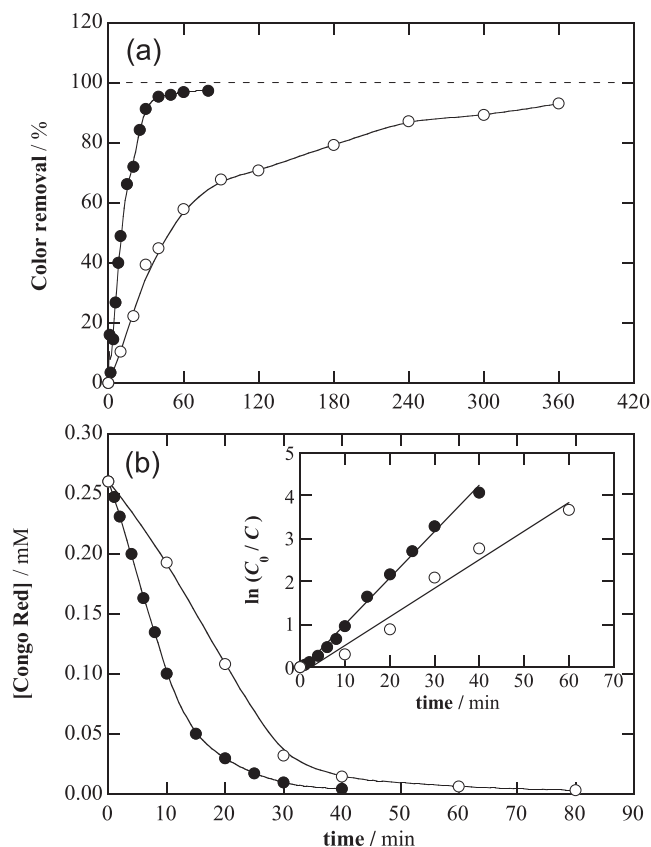


**Fig. 1.** Change of (a) decolorization efficiency and (b) dye concentration with electrolysis time for the treatment of 100 mL of 0.260 mM Congo Red solutions in 0.05 M Na<sub>2</sub>SO<sub>4</sub> at pH 3.0 using a BDD/air- diffusion cell with 3 cm<sup>2</sup> electrodes at 100 mA cm<sup>-2</sup> and 35 °C. Method: (○) Anodic oxidation with electrogenerated H<sub>2</sub>O<sub>2</sub> (AO-H<sub>2</sub>O<sub>2</sub>) and (●) electro-Fenton (EF) or UVA photoelectro-Fenton (PEF) with 0.50 mM Fe<sup>2+</sup> as catalyst. The inset panel of graphic (b) shows the kinetic analysis assuming a pseudo-first-order reaction for Congo Red.

obtained, a pseudo-first-order rate constant (*k*<sub>1</sub>) of 0.066 min<sup>-1</sup> (*R*<sup>2</sup> = 0.975) was found for AO-H<sub>2</sub>O<sub>2</sub>, which was upgraded up to 0.107–0.108 min<sup>-1</sup> (*R*<sup>2</sup> = 0.994) for EF and PEF. This behavior seems feasible because oxidant hydroxyl radicals have so short lifetime that they reach a steady concentration and then, their second-order reaction with the dye behaves as a pseudo-first-order one in all the treatments checked.

Table 1 summarizes the percentage of color removal at 120 min of electrolysis and the *k*<sub>1</sub> values obtained for the treatment of a 0.260 mM Congo Red solution at pH 3.0 and different *j* values. For all the EAOPs, both parameters increased gradually as *j* rose from 16.7 to 100 mA cm<sup>-2</sup>, as expected from the concomitant greater production of BDD(•OH) from the acceleration of Reaction (1) and/or the higher generation of H<sub>2</sub>O<sub>2</sub> by Reaction (2) yielding more quantity of •OH via Fenton's Reaction (4). It is noteworthy that *k*<sub>1</sub> increases linearly with *j* for AO- H<sub>2</sub>O<sub>2</sub> indicating a linear rise of BDD(•OH) to react with the dye. In contrast, the increase in *k*<sub>1</sub> for EF and PEF showed a loss in 18% from linearity, suggesting a loss in homogeneous •OH by the enhancement of its parasitic reactions, as will be discussed below. Results of Table 1 also show the superiority of EF and PEF to decolorize and to remove the dye for all *j* values. This confirms again the higher oxidation ability of •OH in the bulk compared to BDD(•OH) at the anode surface for these EAOPs.

A different relative oxidation ability of EAOPs was found by monitoring the dye mineralization from DOC abatement. Fig. 2a highlights the existence of an induction time near 180 min for beginning to mineralize the 0.260 mM Congo Red solution by AO-H<sub>2</sub>O<sub>2</sub>, only attaining about 40% DOC decay at 360 min. Taking into



**Table 1**

Percentage of color removal, pseudo-first-order rate constant for dye decay, percentage of DOC removal and mineralization current efficiency obtained for the degradation of 100 mL of 0.260 mM Congo Red solutions in 0.05 M Na<sub>2</sub>SO<sub>4</sub> at pH 3.0 using a BDD/air-diffusion cell by different EAOPs at several current densities.

| Methods                          | $j$ /mA cm <sup>-2</sup> | Color removal/% <sup>a</sup> | $k_1$ /min <sup>-1</sup> ( $R^2$ ) | DOC removal/% <sup>b</sup> | MCE/% <sup>b</sup> |
|----------------------------------|--------------------------|------------------------------|------------------------------------|----------------------------|--------------------|
| AO-H <sub>2</sub> O <sub>2</sub> | 16.7                     | 36                           | 0.006 (0.997)                      | 0                          | –                  |
|                                  | 33.3                     | 50                           | 0.014 (0.998)                      | 1                          | –                  |
|                                  | 66.7                     | 67                           | 0.031 (0.983)                      | 27                         | 2.8                |
|                                  | 100                      | 71                           | 0.066 (0.975)                      | 39                         | 2.6                |
| EF <sup>c</sup>                  | 16.7                     | 78                           | 0.022 (0.993)                      | 1                          | –                  |
|                                  | 33.3                     | 95                           | 0.032 (0.994)                      | 54                         | 11                 |
|                                  | 66.7                     | 96                           | 0.050 (0.997)                      | 87                         | 9.0                |
|                                  | 100                      | 100                          | 0.108 (0.994)                      | 92                         | 6.3                |
| PEF <sup>d</sup>                 | 16.7                     | 79                           | 0.021 (0.990)                      | 18                         | 7.3                |
|                                  | 33.3                     | 95                           | 0.033 (0.996)                      | 67                         | 14                 |
|                                  | 66.7                     | 96                           | 0.049 (0.997)                      | 97                         | 10                 |
|                                  | 100                      | 100                          | 0.107 (0.993)                      | 99                         | 6.9                |

<sup>a</sup> Value at 120 min.

<sup>b</sup> Value at 360 min.

<sup>c</sup> With 0.50 mM Fe<sup>2+</sup>.

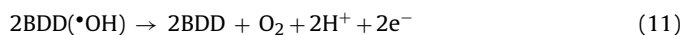
<sup>d</sup> With 0.50 mM Fe<sup>2+</sup> and irradiation under a 6 W UVA light.

account the quick decay of the dye by this method (see Fig. 1b), one can infer the formation of highly recalcitrant products from the attack of BDD(•OH), which are further very slowly transformed into CO<sub>2</sub>. In contrast, the much faster destruction of products by •OH formed from Fenton's Reaction (4) yielded 92% mineralization at the end of EF treatment, whereas the solution was almost totally decontaminated (97% DOC decay) by means of PEF. The superior oxidation power of the PEF can be related to the parallel photolysis of intermediates, including Fe(III)-carboxylate species via Reaction (6), under exposition to UVA light.

The increasing oxidation ability of EAOPs for dye mineralization in the sequence AO-H<sub>2</sub>O<sub>2</sub> < EF < PEF was reflected in the corre-

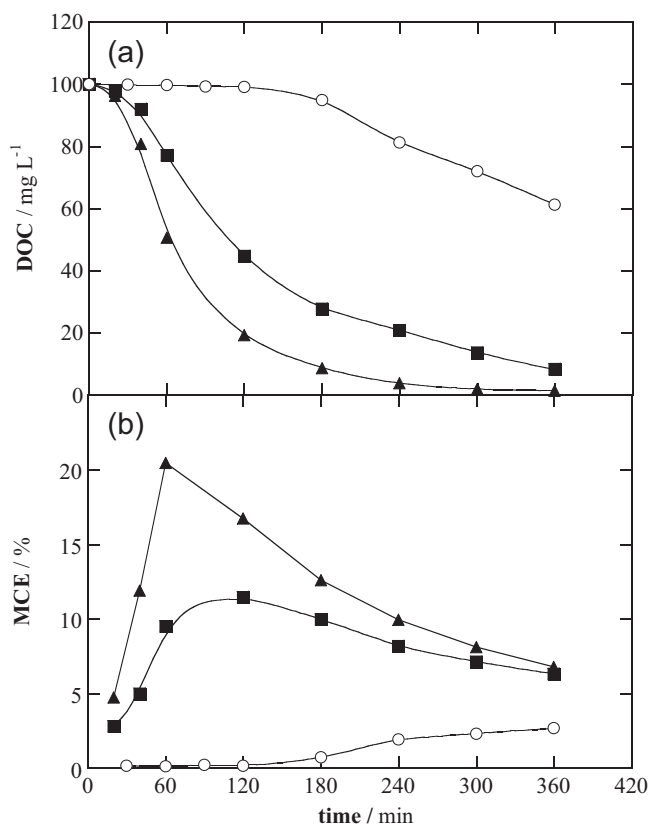
sponding MCE values calculated from Eq. (8). Fig. 2b illustrates that AO-H<sub>2</sub>O<sub>2</sub> only allowed 2.7% of efficiency as maximal, whereas maximum MCE values of 11% and 20% were obtained for EF and PEF, respectively. For long electrolysis times of the two latter processes, the efficiency dropped progressively by two main reasons: (i) the generation of more highly oxidizable products, which are more rapidly photolyzed in SPEF, and (ii) the gradual loss in organic matter [1,4].

Table 1 shows that at 360 min of electrolysis under our experimental conditions, appreciable DOC removals were reached for  $j \geq 66.7$  mA cm<sup>-2</sup> in AO-H<sub>2</sub>O<sub>2</sub> and for  $j \geq 33.3$  mA cm<sup>-2</sup> in EF and PEF. In all cases, the mineralization increased with increasing  $j$  due to the concomitant production of higher amounts of BDD(•OH) and/or •OH, as stated above. Almost total mineralization (97–99% DOC decay) was only achieved using PEF at  $j \geq 66.7$  mA cm<sup>-2</sup>, that is, when enough amounts of both hydroxyl radicals are formed to oxidize the products yielding species that can be photolyzed by UVA irradiation. However, the increase in  $j$  caused a fall in MCE, an opposite tendency to the greater production of BDD(•OH) and/or •OH that mineralized more quickly the Congo Red solution. This loss in efficiency can be related to the acceleration of parasitic reactions consuming both kind of hydroxyl radicals, including the oxidation of BDD(•OH) to O<sub>2</sub> by reaction (11) and the reaction of •OH with Fe<sup>2+</sup> and H<sub>2</sub>O<sub>2</sub> by Reactions (12) and (13), respectively [2–4]. The higher increase in rate of the latter reaction with increasing  $j$  could also explain the drop in linearity of  $k_1$  found for EF and PEF (see Table 1). The faster generation of other weaker oxidants at the BDD anode, like S<sub>2</sub>O<sub>8</sub><sup>2-</sup> ion from Reaction (14) and ozone from Reaction (15) [1], also contributes to less DOC abatement by the drop of BDD(•OH) concentration at the anode surface.



### 3.2. Time course of short carboxylic acids and released inorganic ions by AO-H<sub>2</sub>O<sub>2</sub>, EF and PEF

The above Congo Red solutions degraded by AO-H<sub>2</sub>O<sub>2</sub>, EF and PEF in a stirred BDD/air-diffusion tank reactor at  $j = 100$  mA cm<sup>-2</sup> were analyzed by ion-exclusion HPLC to identify and quantify the generated short-chain aliphatic carboxylic acids. These



**Fig. 2.** Variation of (a) DOC and (b) mineralization current efficiency for the trials of Fig. 1. Method: (○) AO-H<sub>2</sub>O<sub>2</sub>, (■) EF and (▲) PEF.

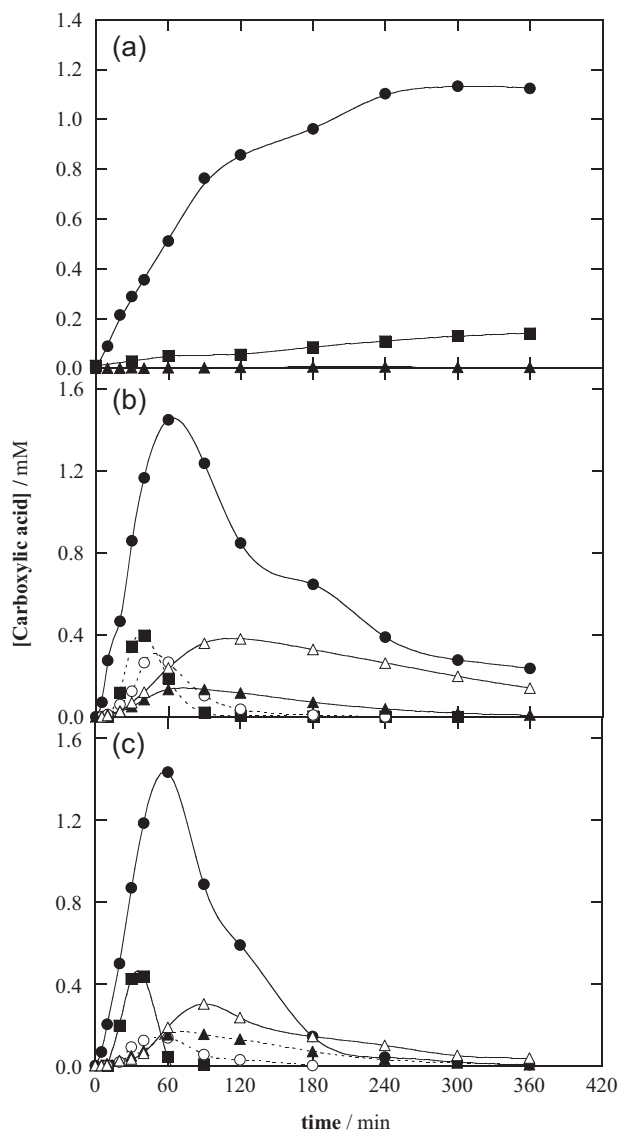


**Fig. 3.** Evolution of the concentration of (●) oxalic, (■) tartaric, (▲) oxamic, (○) tartronic and (△) acetic acids identified during the treatments of Fig. 2 by (a) AO-H<sub>2</sub>O<sub>2</sub>, (b) EF and (c) PEF.

chromatograms displayed well-defined peaks corresponding to oxalic ( $t_r = 7.00$  min), tartronic ( $t_r = 7.92$  min), tartaric ( $t_r = 8.24$  min), oxamic ( $t_r = 9.39$  min) and acetic ( $t_r = 14.96$  min) acids. Tartronic, tartaric and acetic acids are expected to be formed from the successive cleavage of the aromatic moieties of intermediates [4,7,9,24–29,31]. Oxidation of these acids leads to oxalic acid [25–29,31,35–37], whereas oxamic acid can be produced from precedent amino derivatives. Note that oxalic and oxamic acids are ultimate compounds that are directly transformed into CO<sub>2</sub> [2,34].

Fig. 3a highlights that in AO-H<sub>2</sub>O<sub>2</sub>, oxalic acid was largely accumulated up to 1.12 mM at 360 min, whereas oxamic acid was much only accumulated up to 0.0034 mM. The concentration of both acids represented 27.7 mg CL<sup>-1</sup>, which corresponded to about 45% of the DOC of the final treated solution (see Table 1). This means that short-chain carboxylic acids, primordially oxalic acid, are important oxidation products of the degradation process of Congo Red although other unidentified compounds, even more persistent to the attack of BDD(•OH), remain at the end of AO-H<sub>2</sub>O<sub>2</sub>. For EF, Fig. 3b depicts a larger formation of all carboxylic acids with a quick decay of their Fe(III)-complexes by the attack of BDD(•OH) and/or •OH.

Oxalic acid was again the most generated acid, reaching a maximal of 1.45 mM at 60 min and decaying to 0.23 mM at 360 min. Similarly, 0.13 and 0.01 mM of acetic and oxamic acids, respectively, were detected at the end of EF. All these acids gave about 9 mg CL<sup>-1</sup>, just corresponding to the DOC of the final solution, indicating that all the oxidation products can be effectively mineralized by •OH and converted into short-chain carboxylic acids as final species. In the case of PEF, Fig. 3c shows that all the carboxylic acids were accumulated at the same extent as in EF, but it decayed more rapidly owing to the photodecarboxylation of their Fe(III)-carboxylate complexes, thereby enhancing DOC removal and making PEF as the most potent EAOP. Note that at the end of PEF, about 1 mg CL<sup>-1</sup> still remained in the solution mainly due to the presence of Fe(III)-acetate complexes, which are more slowly photolyzed than Fe(III)-oxalate and Fe(III)-oxamate ones [25].

NH<sub>4</sub><sup>+</sup>, NO<sub>3</sub><sup>-</sup> and SO<sub>4</sub><sup>2-</sup> ions coming from the mineralization of the N and S heteroatoms of Congo Red were quantified during the above assays at 100 mA cm<sup>-2</sup> and 35 °C by ion chromatography and the data obtained are presented in Fig. 4a–c, respectively. Results of Fig. 4a and b highlight that NO<sub>3</sub><sup>-</sup> ion was released in much larger proportion than NH<sub>4</sub><sup>+</sup> ion in most cases. At 360 min of treatment, for example, NO<sub>3</sub><sup>-</sup> concentrations of 0.064 mM (4.1% of initial N), 0.158 mM (10.1% of initial N) and 0.229 mM (14.7% of initial N) were obtained for AO-H<sub>2</sub>O<sub>2</sub>, EF and PEF, respectively, whereas NH<sub>4</sub><sup>+</sup> contents of 0.073 mM (4.7% initial N), 0.088 mM (5.6% of initial N) and 0.104 mM (6.7% of initial N) were found. Taking into account these data along with the oxamic acid concentration at the end of processes (see Fig. 3), the N content of the final solutions was only of 2.00, 3.57 and 4.73 mg L<sup>-1</sup> for AO-H<sub>2</sub>O<sub>2</sub>, EF and PEF, respectively, in good agreement with 2.10, 4.80 and 4.91 mg L<sup>-1</sup> experimentally determined by TN analysis. The major discrepancy of 1.03 mg L<sup>-1</sup> was found in the case of EF, suggesting that its final solution still contained unidentified N-derivatives that can be removed in PEF. These results demonstrate that all the EAOPs give a major loss of the initial N (21.84 mg L<sup>-1</sup>) as volatile N-compounds, probably N<sub>x</sub>O<sub>y</sub> and N<sub>2</sub>. In contrast, Fig. 4c reveals a final SO<sub>4</sub><sup>2-</sup> concentration of 0.421 mM (80.8% of initial S) for AO-H<sub>2</sub>O<sub>2</sub>, 0.496 mM (95.4% of initial S) for EF and 0.520 mM (100% of initial S) for PEF. All the EAOPs then allow the release of initial S as SO<sub>4</sub><sup>2-</sup> ion, completely if the solution is almost totally mineralized in PEF, but partially in AO-H<sub>2</sub>O<sub>2</sub> and EF since some intermediates with lateral sulfonic groups are not destroyed.

### 3.3. SPEF treatment of acidic aqueous solutions of Congo Red in a solar flow plant. Optimization of operating variables

Since the study performed in a stirred tank reactor showed that the photo-assisted PEF process is the most potent EAOP for the degradation of Congo Red we extended the treatment to the SPEF process using a 2.5 L solar flow plant to check its viability at industrial scale. The plant contained a Pt/air-diffusion cell which needs a much lower  $E_{\text{cell}}$  for a given  $j$  compared to a BDD/air-diffusion one, thereby making the SPEF treatment more cost-effective. Several series of trials were carried out to optimize important operating variables like applied  $j$  and dye and Fe<sup>2+</sup> concentrations. In all these assays, the effluent pH remained practically constant, slightly decreasing from 3.0 to approximately 2.7–2.8 during the 4 h of electrolysis, reason for which it was not regulated.

A first series of experiments was made by electrolyzing a 0.260 mM Congo Red solution with 0.05 M Na<sub>2</sub>SO<sub>4</sub> and 0.50 mM Fe<sup>2+</sup> by varying  $j$  between 50 and 150 mA cm<sup>-2</sup>. Fig. 5a depicts a very low color removal operating a 50 mA cm<sup>-2</sup>, only reaching 45% decolorization in 150 min. At this low  $j$ , the amounts of generated Pt(•OH) and •OH from Reactions (1) and (4), respectively, are then not high enough to efficiently destroy the dye and its colored aromatic products. In contrast, the acceleration of

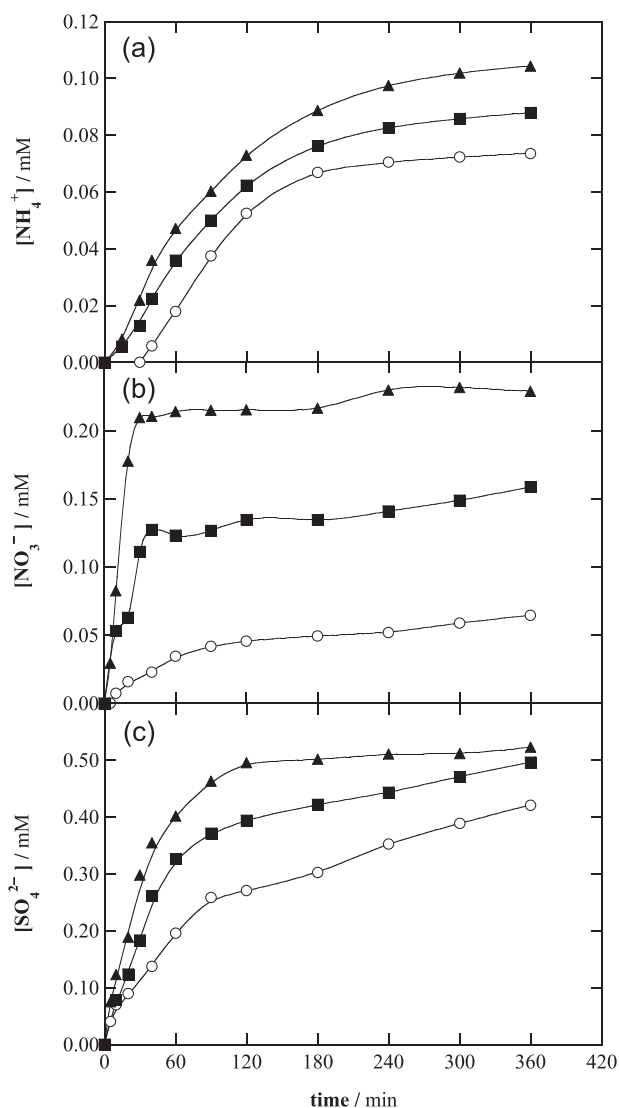


**Fig. 4.** Time-course of the concentration of (a) ammonium, (b) nitrate and (c) sulfate ions during the mineralization processes shown in Fig. 2 by (○) AO-  $\text{H}_2\text{O}_2$ , (■) EF and (▲) PEF.

Reactions (1), (2) and (4) at  $100 \text{ mA cm}^{-2}$  and their much higher enhancement at  $150 \text{ mA cm}^{-2}$  produced much more quantity of both radicals with ability to completely decolorize the solution at 150 and 120 min, respectively. Fig. 5b shows that the abatement of Congo Red was much faster than solution decolorization, disappearing at shorter times of 120, 60 and 40 min for 50, 100 and  $150 \text{ mA cm}^{-2}$ . This confirms the generation of colored aromatic products that react more hardly with generated hydroxyl radicals. As can be seen in the inset panel of Fig. 5b, the reaction of Congo Red with  $\text{Pt}(\bullet\text{OH})$  and mainly  $\bullet\text{OH}$  obeyed a pseudo-first-order reaction with increasing  $k_1$  values of  $0.023 \text{ min}^{-1}$  ( $R^2 = 0.990$ ) for  $50 \text{ mA cm}^{-2}$ ,  $0.064 \text{ min}^{-1}$  ( $R^2 = 0.998$ ) for  $100 \text{ mA cm}^{-2}$  and  $0.081 \text{ min}^{-1}$  ( $R^2 = 0.995$ ) for  $150 \text{ mA cm}^{-2}$  due to the concomitant production of more amounts of both radicals. On the other hand, DOC was poorly reduced at  $50 \text{ mA cm}^{-2}$ , only by 44% after 240 min of electrolysis, whereas the effluent was almost totally mineralized (97–98% DOC abatement) at similar rate by applying 100 and  $150 \text{ mA cm}^{-2}$  during the same time, as can be seen in Fig. 6a. This behavior was also reflected in the MCE values depicted in Fig. 6b. The process showed the highest efficiency at the lowest  $j = 50 \text{ mA cm}^{-2}$  only up to 120 min, after which and due to its very slow mineralization the use of  $100 \text{ mA cm}^{-2}$  was more efficient

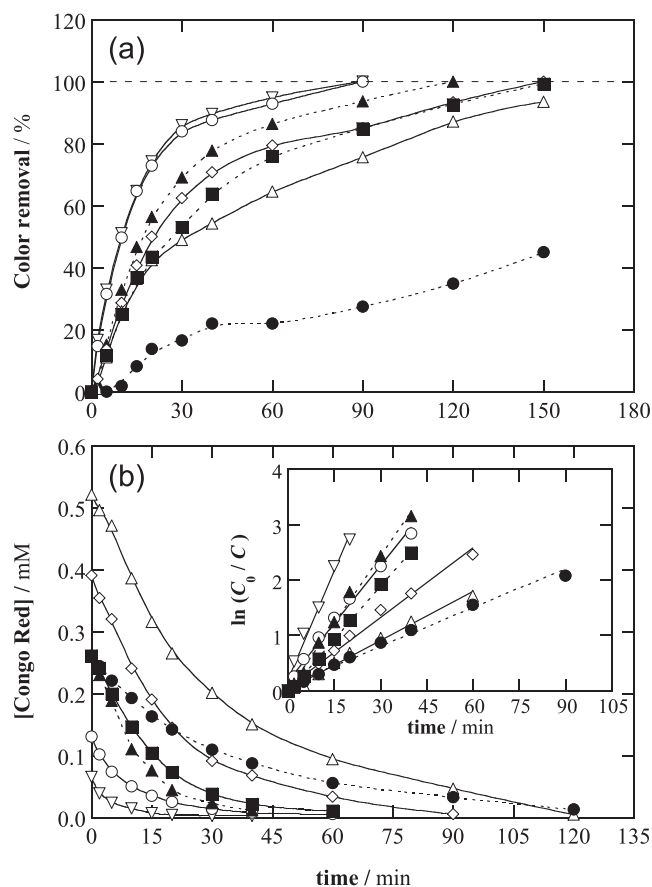


**Fig. 5.** Effect of current density and dye concentration on (a) percentage of color removal and (b) dye concentration abatement for the SPEF treatment of 2.5 L of Congo Red solutions in 0.05 M  $\text{Na}_2\text{SO}_4$  with 0.50 mM  $\text{Fe}^{2+}$  at pH 3.0 and  $35^\circ\text{C}$  using a solar flow plant with a Pt/air-diffusion reactor with  $20 \text{ cm}^2$  electrodes coupled to a planar solar photoreactor of 600 mL irradiation volume at liquid flow rate of  $200 \text{ L h}^{-1}$ . Experimental conditions: 0.260 mM dye at (●)  $50 \text{ mA cm}^{-2}$ , (■)  $100 \text{ mA cm}^{-2}$  and (▲)  $150 \text{ mA cm}^{-2}$ ; (○) 0.065 mM, (□) 0.130 mM, (◇) 0.390 mM and (△) 0.520 mM dye at  $150 \text{ mA cm}^{-2}$ . The inset panel of graphic (b) presents the kinetic analysis considering that Congo Red verifies a pseudo-first-order reaction.

with an MCE near 49% practically during all the SPEF treatment. Lower MCE values were obtained at  $150 \text{ mA cm}^{-2}$  as a result of the increase in rate of parasitic Reactions like (12) and (13) that caused a lower relative generation of  $\bullet\text{OH}$  with the consequent loss in efficiency. Fig. 6c shows that the  $\text{EC}_{\text{DOC}}$  increased gradually with increasing  $j$ , with quite similar values for 50 and  $100 \text{ mA cm}^{-2}$ . For the latter  $j$ , a constant energy consumption of about  $0.35 \text{ kWh (g DOC)}^{-1}$  was found up to 180 min, raising to  $0.45 \text{ kWh (g DOC)}^{-1}$  at the end of treatment. All these findings indicate that the optimum  $j$  for Congo Red degradation in the solar flow plant is  $100 \text{ mA cm}^{-2}$ , which allows total decolorization and mineralization with a good efficiency and relatively low energy consumption.

A subsequent study was carried out with effluents containing dye contents in the range 0.065–0.520 mM with 0.50 mM  $\text{Fe}^{2+}$  and operating at  $150 \text{ mA cm}^{-2}$ . Fig. 5a illustrates the existence of a gradual drop in decolorization efficiency with the growth of Congo Red attaining, for example, total color removal in 90 min for 0.065 mM but only 93% decolorization after 150 min of SPEF treatment for 0.520 mM. This trend can be simply ascribed to the destruction of a smaller proportion of organics by a similar amount of generated  $\text{Pt}(\bullet\text{OH})$  and  $\bullet\text{OH}$  at greater organic load. The same behavior can be observed in Fig. 5b for the abatement of dye concentration, although, as expected, less time was needed for its complete disappearance, which increased from 20 min at 0.065 mM to 120 min at 0.520 mM. This leads to the concomitant decrease in  $k_1$

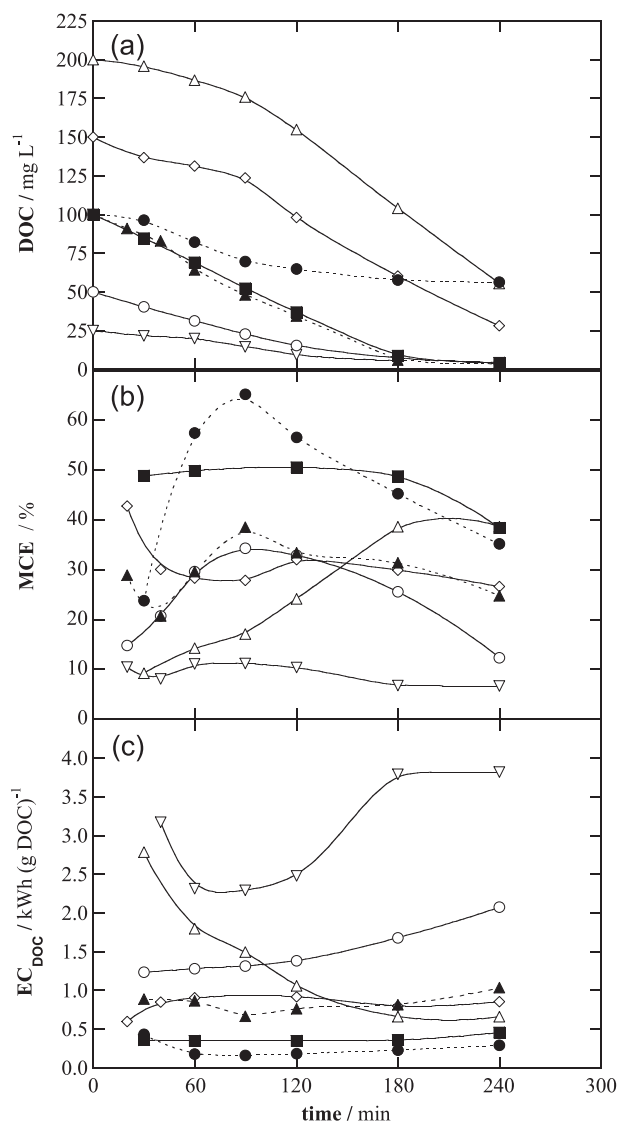


**Fig. 6.** Variation of (a) DOC, (b) mineralization current efficiency and (c) energy consumption per unit DOC mass for the same solutions of Fig. 5. Experimental conditions: 0.260 mM dye at (●) 50 mA cm<sup>-2</sup>, (■) 100 mA cm<sup>-2</sup> and (▲) 150 mA cm<sup>-2</sup>; (▽) 0.065 mM, (○) 0.130 mM, (◇) 0.390 mM and (△) 0.520 mM dye at 150 mA cm<sup>-2</sup>.

from 0.131 to 0.029 min<sup>-1</sup>, respectively, as obtained from the excellent linear correlations for a pseudo-first-order kinetics shown in the inset panel of Fig. 5b. This tendency has also been reported for the decay of monoazo dyes [27,31,37] and can be explained by the progressive loss of the steady content of hydroxyl radicals to attack the Congo Red since a higher amount of them destroys the oxidation products formed. Fig. 6a shows that good mineralization degrees were obtained up to 0.260 mM, whereas DOC was more poorly reduced by 81% for 0.390 mM and by 73% for 0.520 mM. The corresponding MCE values shown in Fig. 6b rose from 0.065 to 0.260 mM, indicating that the presence of more organic matter promotes its reaction with more quantities of Pt(•OH) and •OH, then decelerating the parasitic reactions of these radicals. However, the MCE values for the higher concentrations of 0.390 and 0.520 mM were usually lower than those calculated for 0.260 mM and presented an irregular trend by two reasons: (i) the low DOC decay at short times and (ii) the quicker mineralization at long times, indicating the difficulty of the oxidation of high organic loads. In view of this behavior, Fig. 6c depicts that the lower EC<sub>DOC</sub> values were found for 0.260 mM, at least up to 150–180 min of treatment.

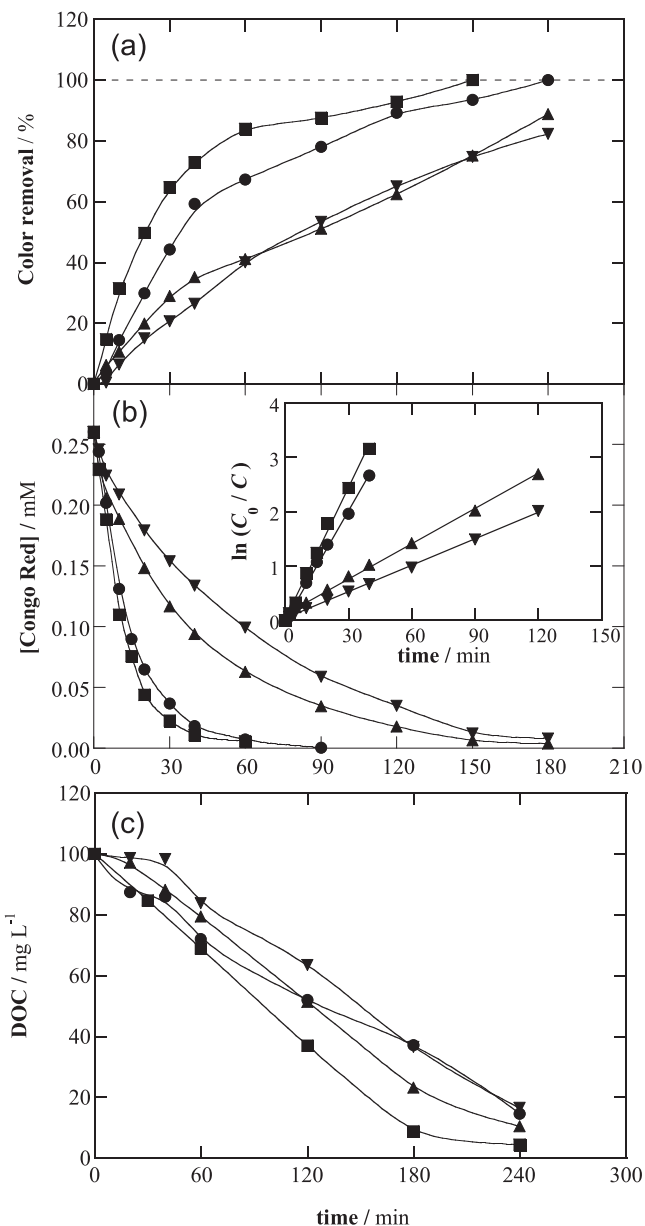


**Fig. 7.** Influence of catalyst concentration on (a) decolorization efficiency, (b) dye concentration decay and (c) DOC removal vs. electrolysis time for the SPEF degradation of 2.5 L of 0.260 mM Congo Red solutions in 0.05 M Na<sub>2</sub>SO<sub>4</sub> at pH 3.0 using a solar flow plant at (a,b) 150 mA cm<sup>-2</sup> and (c) 100 mA cm<sup>-2</sup>, 35 °C and liquid flow rate of 200 L h<sup>-1</sup>. Fe<sup>2+</sup> content: (●) 0.25 mM, (■) 0.50 mM, (▲) 1.0 mM and (▼) 2.0 mM. The kinetic analysis considering a pseudo-first-order reaction for Congo Red is given in the inset panel of graphic (b).

According to these findings, this concentration of Congo Red can be taken as optimal for the SPEF process under our experimental conditions.

The influence of Fe<sup>2+</sup> concentration, which is a key parameter for limiting •OH production from Fenton's Reaction (4), was investigated for a 0.260 mM Congo Red solution with 0.25–2.0 mM Fe<sup>2+</sup> at *j* values of 100 and 150 mA cm<sup>-2</sup>. As an example, Fig. 7a and b illustrates that at 150 mA cm<sup>-2</sup> the quickest decolorization and dye decay was attained for 0.50 mM Fe<sup>2+</sup>. These parameters were enhanced by passing from 0.25 to 0.50 mM Fe<sup>2+</sup>, but underwent a progressive decay when Fe<sup>2+</sup> content further rose up to 2.0 mM. The good linear straight lines found assuming a pseudo-first-order kinetics for dye concentration abatement are presented in the inset panel of Fig. 7b and are indicative of the generation of a



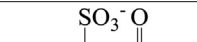
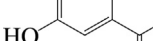
**Table 2**

Aromatic intermediates detected by LC–MS during the SPEF treatment of 2.5 L of a 0.260 mM Congo Red solution in 0.05 M Na<sub>2</sub>SO<sub>4</sub> with 0.50 mM Fe<sup>2+</sup> at pH 3.0 and 100 mA cm<sup>−2</sup>.

| Compound | Molecular structure | Number of –OH added | m/z  |
|----------|---------------------|---------------------|--|
| 1        |                     | – 1 2               | 651 <sup>a</sup> 325 <sup>b</sup> 667 <sup>a</sup> 333 <sup>b</sup> 341 <sup>b</sup> |
| 2        |                     | –                   | 340 <sup>b</sup>   |
| 3        |                     | – 2                 | 318 <sup>b</sup> 334 <sup>b</sup>  |
| 4        |                     | –                   | 416 <sup>a</sup>   |
| 5        |                     | –                   | 337 <sup>a</sup>   |
| 6        |                     | 1 3                 | 354 <sup>a</sup> 386 <sup>a</sup>  |
| 7        |                     | 2                   | 480 <sup>a</sup>   |

Table 2 (Continued)

| Compound | Molecular structure | Number of—OH added | m/z                               |
|----------|---------------------|--------------------|-----------------------------------|
| 8        |                     | –                  | 183 <sup>a</sup>                  |
| 9        |                     | 2                  | 216 <sup>a</sup>                  |
| 10       |                     | – 2                | 185 <sup>a</sup> 217 <sup>a</sup> |
| 11       |                     | 3                  | 291 <sup>a</sup>                  |
| 12       |                     | –                  | 138 <sup>a</sup>                  |
| 13       |                     | –                  | 156 <sup>a</sup>                  |
| 14       |                     | 2 3                | 269 <sup>a</sup> 285 <sup>a</sup> |
| 15       |                     | – 1                | 297 <sup>a</sup> 313 <sup>a</sup> |
| 16       |                     | –                  | 233 <sup>a</sup>                  |
| 17       |                     | –                  | 223 <sup>a</sup>                  |
| 18       |                     | –                  | 291 <sup>a</sup>                  |
| 19       |                     | –                  | 195 <sup>a</sup>                  |
| 20       |                     | –                  | 305 <sup>a</sup>                  |

| Compound | Molecular structure   | Number of—OH added | <i>m/z</i>                        |
|----------|---|--------------------|-----------------------------------|
| 21       |  | – 1                | 261 <sup>a</sup> 277 <sup>a</sup> |
| 22       |  | – 2                | 165 <sup>a</sup> 197 <sup>a</sup> |

b  $z = -2$

The above results confirm the viability of using SPEF for the treatment of waters polluted with Congo Red. Optimum operating conditions were found for a 0.260 mM dye effluent in the presence of 0.50 mM  $\text{Fe}^{2+}$  and by applying  $100 \text{ mA cm}^{-2}$ , where almost total mineralization was reached in 240 min with a good efficiency of near 49% and energy consumption of  $0.45 \text{ kWh (g DOC)}^{-1}$ . Application of other technologies gave poorer decontamination results. For instance, the use of ozonation to destroy 0.430 mM Congo Red at pH 8.7 yielded quick decolorization following a pseudo-

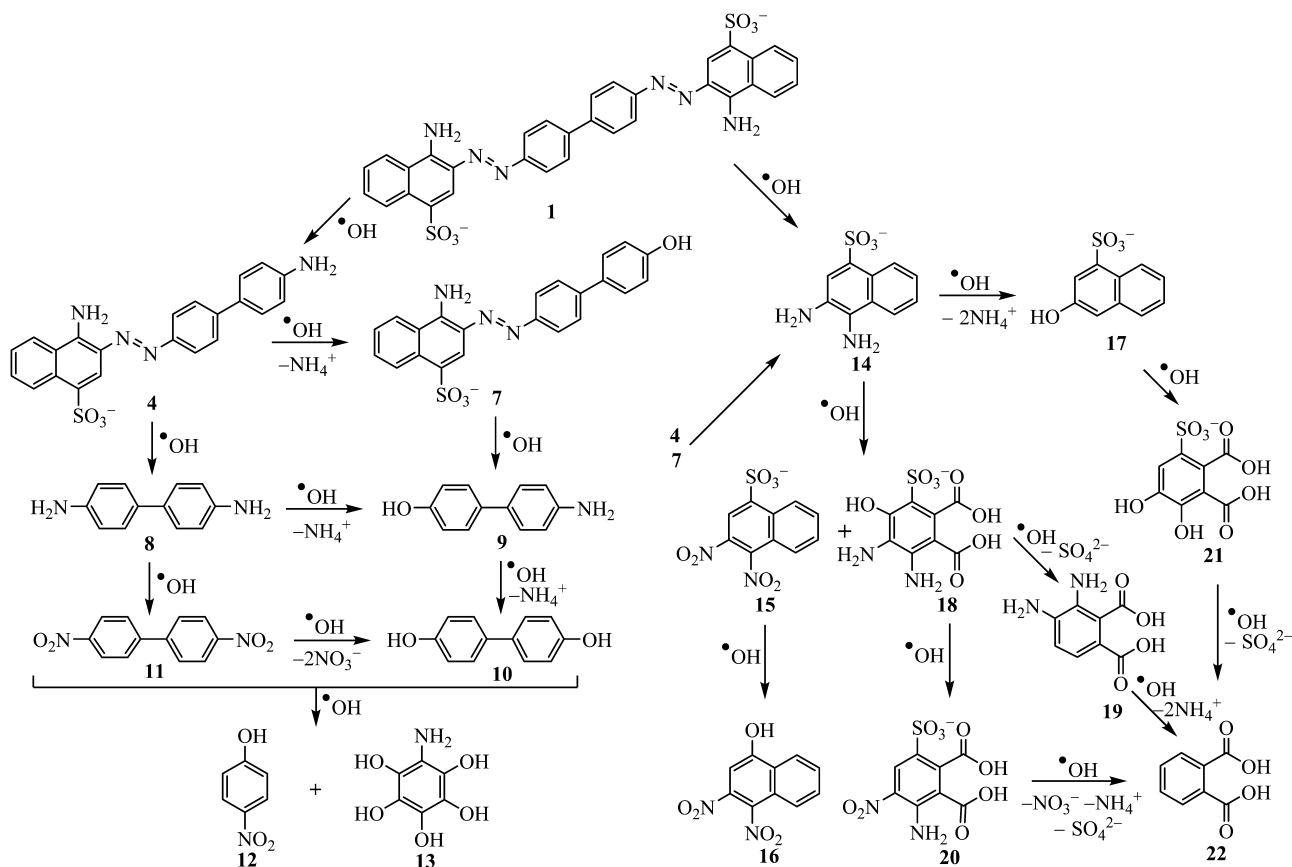


**Fig. 8.** Proposed general reaction sequence for the initial degradation of Congo Red by SPEF.

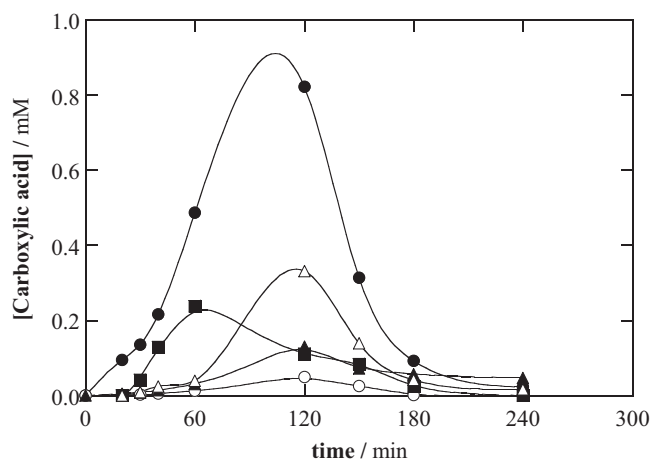


**Fig. 9.** Evolution of the concentration of (●) oxalic, (■) tartaric, (▲) oxamic, (○) tartronic and (△) acetic acids detected during the SPEF degradation of 2.5 L of a 0.260 mM Congo Red, 0.05 M  $\text{Na}_2\text{SO}_4$  and 0.50 mM  $\text{Fe}^{2+}$  solution of pH 3.0 in a solar flow plant at  $100 \text{ mA cm}^{-2}$ ,  $35^\circ\text{C}$  and liquid flow rate of  $200 \text{ L h}^{-1}$ .

first-order decay, but COD and TOC were only reduced by 54% and 32%, respectively [47]. Similarly, wet peroxide oxidation only allowed 58% COD removal of Congo Red solutions at optimum pH 7 and  $90^\circ\text{C}$  after adding  $\text{H}_2\text{O}_2$  and  $1 \text{ g L}^{-1}$  of Fe exchanged commercial Y zeolite as catalyst [48]. Total decolorization from 20 to 60 min, always obeying a pseudo-first order removal, was found for the photo-Fenton treatment of increasing Congo Red content from 0.120 to 0.503 mM using an iron-pillary clay as catalyst at pH 3 under a 100 W UVA irradiation, but with much slower mineralization [49].  $\text{TiO}_2/\text{UV}$  photocatalysis of 0.070 mM Congo Red solution only led to 82% decolorization with TOC abatement as low as 34% [50].

#### 3.4. Identification and evolution of products in the SPEF process

Samples of the short-time treated dye solution under optimum SPEF conditions were withdrawn and analyzed by LC–MS. Table 2 collects the 21 aromatic intermediates and 13 hydroxylated derivatives, apart from the starting dye (1), detected by this technique. An initial reaction sequence can be envisaged from these products. Thus, 1 can be mono- or dihydroxylated, nitrified to yield 2 or deaminated with hydroxylation to give 3. The chromophore group of all these primary intermediates is quite similar to the dye and may be a part of the colored aromatic products that prolong its decolorization process, as pointed out above. The cleavage of one  $-\text{N}=\text{N}-$  bond of 1 produces the monoazo 4, which is subsequently desulfonated leading to 5, followed by deamination with hydroxylation to form 6. Parallel nitrification and deamination with hydroxylation of 4 gives 7. The cleavage of the  $-\text{N}=\text{N}-$  bond of 4 originates 4,4'-diaminobiphenyl (8), which undergoes successive deamination with hydroxylation reactions to yield 9 and 10, which can also be produced from the breaking of the  $-\text{N}=\text{N}-$  bond of 7. Nitrification of the two amino groups of 8 leads to 11, whereas the cleavage of the C–C bond between its two benzenic rings originates *p*-nitrophenol (12) and pentahydroxyaniline (13). On the other hand, the cleavage of one or two  $-\text{N}=\text{N}-$  bonds released the naphthalene derivative 14, which is further nitrified, desulfonated or deaminated with hydroxylation to form 15, 16 or 17, respectively. Subsequent oxidation of 14 and 17 leads to several phthalic acid derivatives like 18–21 containing amino, nitro, hydroxyl and/or sulfonic groups linked to the benzenic ring [35]. The loss of all these groups gives phthalic acid (22). A plausible general reaction scheme involving the main aromatic intermediates is shown in Fig. 8.

The above aromatic intermediates are expected to be formed in AO- $\text{H}_2\text{O}_2$ , EF and PEF processes since generated hydroxyl radicals are the main oxidizing agents in all the EAOPs tested. Further destruction of these compounds leads to the short-linear aliphatic carboxylic acids detected in such processes, which were also produced in the SPEF one. Fig. 9 depicts the evolution of tartaric, tartronic, acetic, oxalic and oxamic acids during the SPEF process under optimum conditions. As in the case of PEF in stirred tank reactor, all these acids practically disappeared at the end of SPEF when almost overall mineralization was attained. Oxalic acid was again the most largely accumulated final compound, up to 0.8–0.9 mM, rapidly being transformed into  $\text{CO}_2$  by the potent photolytic action of UV intensity of sunlight on its Fe(III) complexes. It was also corroborated the release of  $\text{NH}_4^+$ ,  $\text{NO}_3^-$  and  $\text{SO}_4^{2-}$  ions during the optimum SPEF degradation of the 0.260 mM Congo Red solution, with similar behavior to that described above for the PEF treatment in stirred tank reactor.

## 7. Conclusions

It has been demonstrated that a photo-assisted electrochemical method based on Fenton's reaction chemistry like PEF is more potent for the degradation of 0.260 mM Congo Red at pH 3.0 than AO- $\text{H}_2\text{O}_2$  and EF using a stirred BDD/air-diffusion tank reactor. Faster decolorization efficiency and dye concentration decay were found for PEF, reaching an almost total mineralization after 360 min at  $j \geq 66.7 \text{ mA cm}^{-2}$ . The relative oxidation power of the EAOPs rose in the sequence AO- $\text{H}_2\text{O}_2 < \text{EF} < \text{PEF}$ . This is due to the faster reaction of  $\cdot\text{OH}$  in the bulk than BDD( $\cdot\text{OH}$ ) at the anode surface with the dye and its products in EF, along with the parallel photolysis of species by UVA light in PEF. The increase in  $j$  promoted the decolorization, dye decay and mineralization in all the EAOPs, but with a loss of MCE values and an enhancement of the energy consumption. Congo Red abatement always obeyed a pseudo-first-order kinetics. Tartaric, tartronic, acetic, oxalic and oxamic acids were detected as final carboxylic acids. These compounds were poorly removed in AO- $\text{H}_2\text{O}_2$ , more rapidly destroyed in EF and almost completely mineralized in PEF as a result of the quick photodecarboxylation of their Fe(III) complexes. The initial S of the dye was transformed into  $\text{SO}_4^{2-}$  ion, whereas its initial N was mainly released as *N*-volatile compounds and mineralized to  $\text{NO}_3^-$  ion and in lesser extent to  $\text{NH}_4^+$  ion. The study of the Congo Red degradation was extended to a 2.5 L solar flow plant, showing the viability of SPEF treatment at industrial scale. This process was optimal for 0.260 mM of the dye with 0.50 mM  $\text{Fe}^{2+}$  at  $100 \text{ mA cm}^{-2}$ , reaching an almost total mineralization in 240 min with a MCE near 49% and energy consumption of  $0.45 \text{ kWh (g DOC)}^{-1}$ . Up to 21 aromatic intermediates and 13 hydroxylated derivatives, including diazo, monoazo, biphenyl, benzene, naphthalene and phthalic acid compounds, were identified by LC–MS. The same carboxylic acids and released  $\text{NH}_4^+$ ,  $\text{NO}_3^-$  and  $\text{SO}_4^{2-}$  ions, with similar evolution to that found in PEF in a stirred tank reactor, were also obtained by SPEF using a solar flow plant.

## Acknowledgments

The authors thank MINECO (Spain) for economical support under project CTQ2013-48897-C2-1-R, co-financed by FEDER. S. Solano acknowledges her Doctoral fellowship by the Brazilian program Ciências sem Fronteiras – CNPq (246606/2012-6) and S. Garcia-Segura thanks the Doctoral grant awarded from MEC (Spain).



## References

- [1] M. Panizza, G. Cerisola, *Chem. Rev.* 109 (2009) 6541–6569.
- [2] E. Brillas, I. Sirés, M.A. Oturan, *Chem. Rev.* 109 (2009) 6570–6631.
- [3] I. Sirés, E. Brillas, M.A. Oturan, M.A. Rodrigo, M. Panizza, *Environ. Sci. Pollut. Res.* 21 (2014) 8336–8367.
- [4] E. Brillas, C.A. Martínez-Huitle, *Appl. Catal. B* 166–167 (2015) 603–643.
- [5] G.R. de Oliveira, C.K.C. de Araújo, C.A. Martínez-Huitle, D.R. da Silva, *Curr. Org. Chem.* 16 (2012) 1957–1959.
- [6] L. Feng, E.D. van Hullebusch, M.A. Rodrigo, G. Esposito, M.A. Oturan, *Chem. Eng. J.* 228 (2013) 944–964.
- [7] B. Boye, P.A. Michaud, B. Marselli, M.M. Dieng, E. Brillas, C. Comninellis, *New Diamond Front. Carbon Technol.* 12 (2002) 63–72.
- [8] B. Marselli, J. García-Gomez, P.A. Michaud, M.A. Rodrigo, C. Comninellis, *J. Electrochem. Soc.* 150 (2003) D79–D83.
- [9] C. Flox, J.A. Garrido, R.M. Rodríguez, F. Centellas, P.L. Cabot, C. Arias, E. Brillas, *Electrochim. Acta* 50 (2005) 3685–3692.
- [10] C. Flox, C. Arias, E. Brillas, A. Savall, K. Groenen-Serrano, *Chemosphere* 74 (2009) 1340–1347.
- [11] L. Ciriaco, C. Anjo, J. Correia, M.J. Pacheco, A. Lopes, *Electrochim. Acta* 54 (2009) 1464–1472.
- [12] E. Brillas, S. García-Segura, M. Skoumal, C. Arias, *Chemosphere* 79 (2010) 605–612.
- [13] E. Tsantaki, T. Velegriaki, A. Katsounis, D. Mantzavinos, *J. Hazard. Mater.* 207–208 (2012) 91–96.
- [14] M.G. Tavares, L.V.A. da Silva, A.M.S. Solano, J. Tonholo, C.A. Martínez-Huitle, C.L.P.S. Zanta, *Chem. Eng. J.* 204–206 (2012) 141–150.
- [15] N. Oturan, E. Brillas, M.A. Oturan, *Environ. Chem. Lett.* 10 (2012) 165–170.
- [16] M.B. Ferreira, J.H.B. Rocha, J.V. de Melo, C.A. Martínez-Huitle, M.A. Quiroz Alfaro, *Electrocatalysis* 4 (2013) 274–282.
- [17] A. Wang, J. Qu, H. Liu, J. Ru, *Appl. Catal. B: Environ.* 84 (2008) 393–399.
- [18] A. Özcan, M.A. Oturan, N. Oturan, Y. Sahin, *J. Hazard. Mater.* 163 (2009) 1213–1220.
- [19] A. Dhaouadi, N. Adhoum, *J. Electroanal. Chem.* 637 (2009) 33–42.
- [20] M. Panizza, M.A. Oturan, *Electrochim. Acta* 56 (2011) 7084–7087.
- [21] F.E.F. Rêgo, A.M.S. Solano, I.C. da Costa Soares, D.R. da Silva, C.A. Martínez-Huitle, M. Panizza, *J. Environ. Chem. Eng.* 2 (2014) 875–880.
- [22] A. Özcan, Y. Sahin, A.S. Koparal, M.A. Oturan, *J. Electroanal. Chem.* 616 (2008) 71–78.
- [23] A. Khataee, A. Khataee, M. Fathinia, B. Vahid, S.W. Joo, *J. Ind. Eng. Chem.* 19 (2013) 1890–1894.
- [24] E. Brillas, M.A. Baños, S. Camps, C. Arias, P.L. Cabot, J.A. Garrido, R.M. Rodríguez, *New J. Chem.* 28 (2004) 314–322.
- [25] C. Flox, J.A. Garrido, R.M. Rodríguez, P.L. Cabot, F. Centellas, C. Arias, E. Brillas, *Catal. Today* 129 (2007) 29–36.
- [26] E. Guinea, J.A. Garrido, R.M. Rodríguez, P.L. Cabot, C. Arias, F. Centellas, E. Brillas, *Electrochim. Acta* 55 (2010) 2101–2115.
- [27] S. García-Segura, F. Centellas, C. Arias, J.A. Garrido, R.M. Rodríguez, P.L. Cabot, E. Brillas, *Electrochim. Acta* 58 (2011) 303–311.
- [28] C. Ramírez, A. Saldaña, B. Hernández, R. Acero, R. Guerra, S. García-Segura, E. Brillas, J.M. Peralta-Hernández, *J. Ind. Eng. Chem.* 19 (2013) 571–579.
- [29] E. Isarain-Chávez, C. de la Rosa, L.A. Godínez, E. Brillas, J.M. Peralta-Hernández, *J. Electroanal. Chem.* 713 (2014) 62–69.
- [30] G.R. Agladze, G.S. Tsurtsumia, B.-I. Jung, J.-S. Kim, G. Gorelishvili, *J. Appl. Electrochem.* 37 (2007) 375–383.
- [31] F.C. Moreira, S. García-Segura, V.J.P. Vilar, R.A.R. Boaventura, E. Brillas, *Appl. Catal. B* 142–143 (2013) 877–890.
- [32] G.R. Agladze, G.S. Tsurtsumia, B.-I. Jung, J.-S. Kim, G. Gorelishvili, *J. Appl. Electrochem.* 37 (2007) 385–393.
- [33] G.R. Agladze, G.S. Tsurtsumia, B.-I. Jung, J.-S. Kim, G. Gorelishvili, *J. Appl. Electrochem.* 37 (2007) 985–990.
- [34] S. García-Segura, E. Brillas, *Water Res.* 45 (2011) 2975–2984.
- [35] E. Isarain-Chávez, P.L. Cabot, F. Centellas, R.M. Rodríguez, C. Arias, J.A. Garrido, E. Brillas, *J. Hazard. Mater.* 185 (2011) 1228–1235.
- [36] L.C. Almeida, S. García-Segura, N. Bocchi, E. Brillas, *Appl. Catal. B* 103 (2011) 21–30.
- [37] E.J. Ruiz, A. Hernández-Ramírez, J.M. Peralta-Hernández, C. Arias, E. Brillas, *Chem. Eng. J.* 171 (2011) 385–392.
- [38] UNESCO, The United Nations World Water Development Report 4, Volume 1: Managing Water Report under Uncertainty and Risk (2012).
- [39] T. Robinson, G. McMullan, R. Marchant, P. Nigam, *Biores. Technol.* 77 (2001) 247–255.
- [40] V. Khandegar, A.K. Saroha, *J. Environ. Manage.* 128 (2013) 949–963.
- [41] K.P. Sharma, S. Sharma, S.P. Sharma, K. Singh, S. Kumar, R. Grover, P.K. Sharma, *Chemosphere* 69 (2007) 48–54.
- [42] S.M.A.G. Ulson de Souza, E. Forgiarini, A.A. Ulson de Souza, *J. Hazard. Mater.* 147 (2007) 1073–1078.
- [43] M. Faouzi Elahmadi, N. Bensalah, A. Gadri, *J. Hazard. Mater.* 168 (2009) 1163–1169.
- [44] P. Cañizares, R. Paz, C. Sáez, M.A. Rodrigo, *J. Environ. Manage.* 90 (2009) 410–420.
- [45] A. Lahkimi, M.A. Oturan, N. Oturan, M. Chaouch, *Environ. Chem. Lett.* 5 (2007) 35–39.
- [46] C. Flox, P.L. Cabot, F. Centellas, J.A. Garrido, R.M. Rodríguez, C. Arias, E. Brillas, *Chemosphere* 64 (2006) 892–902.
- [47] M. Khadhraoui, H. Trabelsi, M. Ksibi, S. Bouguerra, B. Elleuch, *J. Hazard. Mater.* 161 (2009) 974–981.
- [48] A.K. Kondru, P. Kumar, S. Chand, *J. Hazard. Mater.* 166 (2009) 342–347.
- [49] H.B. Hadjitaief, P. Da Costa, M.E. Galvez, M.B. Zina, *Ind. Eng. Chem. Res.* 52 (2013) 16656–16665.
- [50] A. Mayoufi, M.F. Nsib, A. Houas, *C. R. Chim.* 17 (2014) 818–823.